

Supplementary Information

Soft Electrothermal Actuators using Silver Nanowire Heaters

*Shanshan Yao, Jianxun Cui, Zheng Cui and Yong Zhu**

E-mail: yong_zhu@ncsu.edu

Supplementary Information Available:

1. Heating/Cooling rate of AgNW/PDMS heaters
2. Calibrated emissivity of AgNW/PDMS heaters as a function of temperature
3. Summary of the response time for electrothermal bimorph actuators
4. Calculations of the response time of electrothermal bimorph actuators
5. Equations and calculation details on the bending angle and curvature of the bimorph actuators
6. Summary of the reported performance for bimorph actuators
7. Calculation of the bending curvature using the length and displacement of the actuator
8. Stability of PI/AgNW/PDMS actuators

Supplementary Movies:

- Movie S1: Bending behavior of the PI/AgNW/PDMS actuator (note the speed is at 4X).
Movie S2: Walker crawling on flat ratchet surface
Movie S3: Walker crawling upstairs
Movie S4: Walker crawling downstairs
Movie S5: Gripper: Grab and collect
Movie S6: Gripper: Pick and place

1. Heating/Cooling rate of AgNW/PDMS heaters

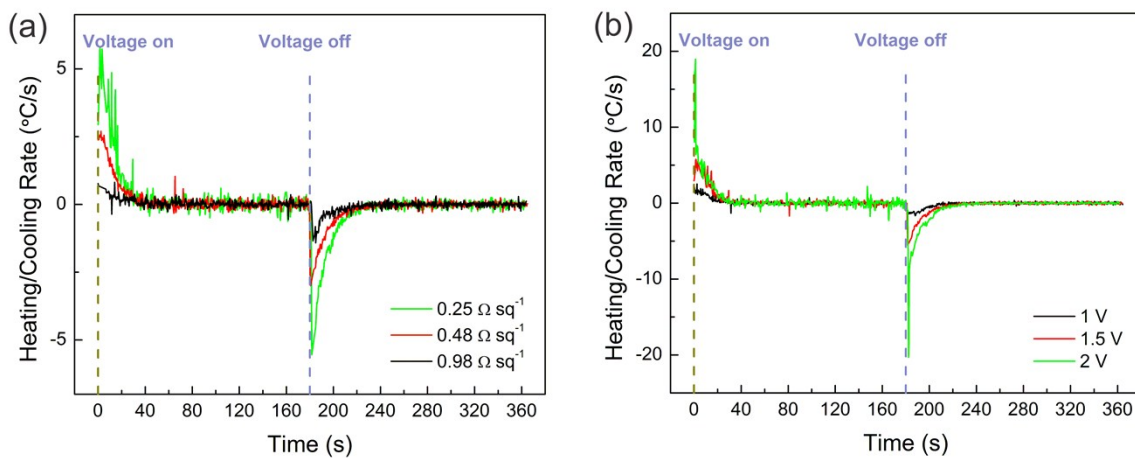


Fig. S1 (a) The heating and cooling rate with respect to different sheet resistance at a constant voltage of 1.5 V. (b) The heating and cooling rate when the heater (sheet resistance of 0.25 Ω sq⁻¹) was subjected to different voltages. The voltage was on for 180 s. The rate was calculated by taking the derivative of the temperature vs. time curves in Fig. 1d and e.

2. Calibrated emissivity of AgNW/PDMS heater as a function of temperature

The emissivity of AgNW/PDMS heater were calibrated using black electrical tape method over the temperature range of RT to 200 °C. AgNW/PDMS heater and black electrical tape were placed adjacent to each other and heated by a hotplate. The temperature of the black electrical tape was recorded as known temperature and the emissivity of the tested material was adjusted until the temperature obtained matched the temperature of the electrical tape. The adjusted emissivity value of AgNW/PDMS which matched the temperature value taken from the electrical tape was used as the emissivity for the material and was plotted as a function of temperature as shown below.

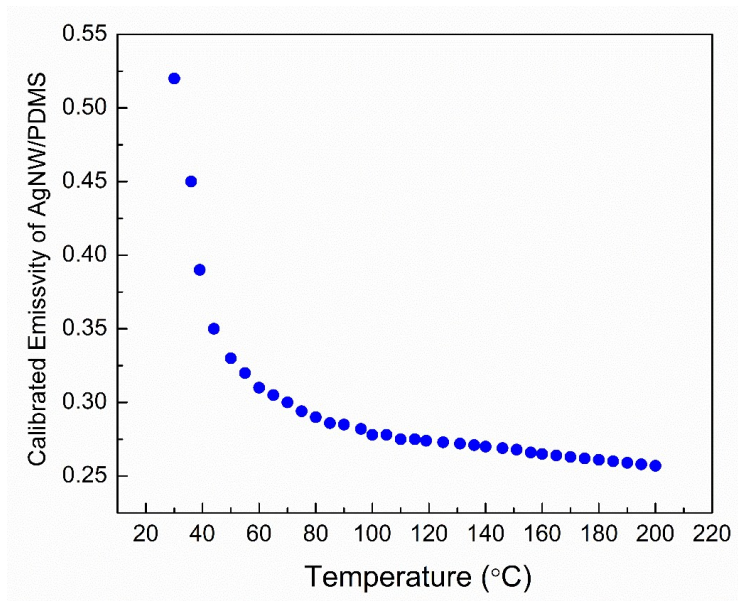


Fig. S2 Calibrated emissivity of the AgNW/PDMS heater as a function of temperature.

3. Summary of the response time for electrothermal bimorph actuators

Table S1 Summary of response time for electrothermal actuators

Materials	Time Taken to Achieve Bending	Bending Curvature	Reference
SACNT/PDMS	~6 s	0.22 cm ⁻¹ †	1
MWCNT-WPU/ MWCNT-Silicone	~50 s	0.29 cm ⁻¹	2
SACNT/PET/BOPP	~30 s	0.41 cm ⁻¹	3
SACNT/BOPP	~10 s	1.03 cm ⁻¹	4
Paper/AgNW/PP	~20 s	1.07 cm ⁻¹	5
Spongy graphene/PDMS	~3 s	1.2 cm ⁻¹	6
PI/AgNW/PDMS	~7 s	1 cm⁻¹	This work
PI/AgNW/PDMS	~10 s	1.25 cm⁻¹	This work
PI/AgNW/PDMS	~40 s	2.6 cm⁻¹	This work

†The curvature was calculated using the length and displacement of the actuator

4. Calculations of the response time of electrothermal bimorph actuators

The temporal response of the actuator is mainly limited by the time taken for the heater to reach the saturated temperature. The input electrical power is converted to the temperature increase of the heater (or actuator) and the heat loss (Q_{loss}) to the surrounding environment:⁷

$$\frac{V^2}{R} dt = cmdT(t) + Q_{loss} dt = cmdT(t) + \varepsilon\sigma A(T(t)^4 - T_0^4)dt + h_C A(T(t) - T_0)dt \quad (1)$$

$$cm = c_h m_h + c_s m_s \quad (2)$$

$$\varepsilon = \varepsilon_h + \varepsilon_s \quad (3)$$

$$h_C = h_{hC} + h_{sC} \quad (4)$$

where V is the applied voltage, R is the resistance, t is time, c is the effective specific heat capacity, c_h and c_s are the specific heat capacity for the heating material and the substrate, respectively, m is the effective mass, m_h and m_s are the mass for the heating material and the substrate, respectively, $T(t)$ is the time dependent temperature, T_0 is the initial temperature, t is the time, ε_h and ε_s are the surface emissivity for the heating material and the substrate, respectively, σ is the Stefan-Boltzmann constant ($5.67 \times 10^{-8} \text{ W m}^{-2} \text{ }^\circ\text{C}^{-4}$), A is the surface area, h_{hC} and h_{sC} are the convection heat transfer coefficients for the heating material and the substrate, respectively.

From the literature, the temporal response of the heater can be described by:^{8,9}

$$T(t) = T_0 + \frac{V^2}{RhA} \left(1 - e^{-\frac{hA}{cm}t}\right) \text{ with } h = h_C + h_R = h_{hC} + h_{sC} + h_{hR} + h_{sR} \quad (5)$$

where h is the total heat transfer coefficient, h_C is the total convection heat transfer coefficient, h_R is the total radiation heat transfer coefficient, h_{hR} and h_{sR} are the radiation heat transfer coefficients for the heater and the substrate, respectively.

Considering a configuration of the heater sandwiched by a layer of PDMS and PI on each side, the temporal response of the temperature can be described by:

$$T(t) = T_0 + \frac{V^2}{Rh'A} (1 - e^{-\frac{h'A}{c'm't}}) = T_0 + \frac{V^2}{Rh'A} (1 - e^{-\frac{t}{\tau}}) \quad \text{with } \tau = \frac{c'm'}{h'A} = \frac{c'\rho d}{h'} \quad (6)$$

$$c'm' = c_h m_h + c_1 m_1 + c_2 m_2 \quad (7)$$

$$h' = h_C' + h_R' = h_{1C} + h_{2C} + h_{1R} + h_{2R} \quad (8)$$

$$c'\rho d = c_h \rho_h d_h + c_1 \rho_1 d_1 + c_2 \rho_2 d_2 \quad (9)$$

where τ is the time constant, h_{1C} and h_{1R} are the convection and radiation heat transfer coefficients for PDMS, respectively, h_{2C} and h_{2R} are the convection and radiation heat transfer coefficients for PI, respectively, c_1 and m_1 are the specific heat capacity and the mass for PDMS, respectively, c_2 and m_2 are the specific heat capacity and the mass for PI, respectively, ρ_h , ρ_1 and ρ_2 are the density for the heater, PDMS and PI, respectively, and d_h , d_1 and d_2 are the thickness for the heater, PDMS and PI, respectively.

Smaller time constant corresponds to faster response. Reduced time constant can be achieved by decreasing the thickness, decreasing the specific heat capacity, decreasing the material density or by increasing the total heat transfer coefficient. In addition, increasing the difference in the coefficient of thermal expansion or optimizing the material properties and geometry of the

actuators can reduce the temperature needed to achieve the same bending curvature, as discussed in “5. Deflection of bimorph actuator”. According to supplementary Eqn (6), reduced response time for the same bending curvature can thus be achieved by decreasing the thickness, decreasing the specific heat capacity, decreasing the material density, decreasing the surface area, or by increasing the input power (I^2/R), increasing the difference in the coefficient of thermal expansion, or by optimizing the total heat transfer coefficient and the ratios of Young’s modulus and thickness of the two layers.

5. Deflection of bimorph actuator

When a bimorph actuator composed of two layers with different material properties is subjected to temperature change, the beam bends to the layer with lower thermal expansion in order to accommodate the mismatch of thermal strain. The resulting bending curvature (k) can be calculated based on Timoshenko's equation:¹⁰

$$k = \frac{1}{r} = \frac{6w_1w_2E_1E_2t_1t_2(t_1+t_2)(\alpha_2-\alpha_1)(T-T_0)}{(w_1E_1t_1^2)^2 + (w_2E_2t_2^2)^2 + 2w_1w_2E_1E_2t_1t_2(2t_1^2 + 3t_1t_2 + 2t_2^2)} \quad (10)$$

where r is the radius of curvature, T_0 is the initial temperature, T is the temperature of the actuator, α_1 and α_2 are the coefficient of thermal expansion for materials 1 and 2, t_1 and t_2 are the thickness of the two layers, w_1 and w_2 are the width of the two layers, E_1 and E_2 are the Young's modulus of the two layers.

When the width of the two layers are identical, the equation can be simplified as

$$k = \frac{1}{r} = \frac{6(\alpha_2 - \alpha_1)(1+m)^2(T-T_0)}{h \left[3(1+m)^2 + (1+mn)\left(m^2 + \frac{1}{mn}\right) \right]} = f(t_1, t_2, E_1, E_2) \Delta T \Delta \alpha \quad (11)$$

$$m = \frac{t_1}{t_2}, \quad n = \frac{E_1}{E_2} \quad (12)$$

where $h = t_1 + t_2$ is the total thickness of the composite, $f(t_1, t_2, E_1, E_2)$ is a function of the thickness and Young's modulus of the two layers. It is obvious that the bending radius (r) and the bending curvature (k) is dependent on the difference in coefficient of the thermal expansion ($\Delta\alpha$), the temperature change (ΔT), the thickness and Young's modulus ratio between the two layers.

In our case, material 1 is PI with a thermal expansion coefficient of $\alpha_{\text{PI}} = 20 \times 10^{-6} \text{ K}^{-1}$ and Young's modulus of 2.5 GPa;¹¹ material 2 is PDMS with a thermal expansion coefficient of $\alpha_{\text{PDMS}} = 310 \times 10^{-6} \text{ K}^{-1}$ and Young's modulus of 1 MPa.¹² The bending curvature as a function of temperature change can thus be calculated and plotted using equation (1) as shown in Fig. 2d.

6. Summary of the reported performance for bimorph actuators

Table S2 Summary of the reported bimorph actuators performance

Materials	Mechanism	Maximum Curvature /Bending Angle	Driven Voltage	Reference
SACNT/PDMS	Electrothermal	0.22 cm ⁻¹ †	40 V, 1.60 V sq ⁻¹	1
MWCNT-WPU/MWCNT-Silicone	Electrothermal	0.29 cm ⁻¹	7 V, 1.17 V sq ⁻¹	2
SACNT/PET/BOPP	Electrothermal	0.41 cm ⁻¹	60 V, 23 V sq ⁻¹	3
SACNT/BOPP	Electrothermal	1.03 cm ⁻¹ /389°	5 V, 1.29 V sq ⁻¹	4
Spongy graphene/PDMS	Electrothermal	1.2 cm ⁻¹	10 V, 0.56 V sq ⁻¹	6
MWNT/PVA	Electrochemical	~90°	8 V, 4.8 V sq ⁻¹	13
Graphene/PDA	Electrochemical	0.37 cm ⁻¹	-	14
PDMS/GNPs	Photothermal	0.62 cm ⁻¹ †	-	15
PC/SWNT	Photothermal	90°	-	16
GO/prGO-PPy	Moisture	330°	-	17
PI/AgNW/PDMS	Electrothermal	2.6 cm⁻¹/720°	4.5 V, 0.20 V sq⁻¹	This work

†The curvature was calculated using the length and displacement of the actuator

7. Calculation of the bending curvature using the length and displacement of the actuator²

Consider an actuator with length of l , displacement at free end after bending of d , bending angle of θ , bending radius of r and curvature of $k = 1/r$ (Fig. S3), we have $\cos\theta = (r-d)/r = 1-dk$ and $\theta = l/r = lk$. Knowing the length and the displacement, the curvature can be derived by solving the following equation: $\cos(lk) = 1-dk$.

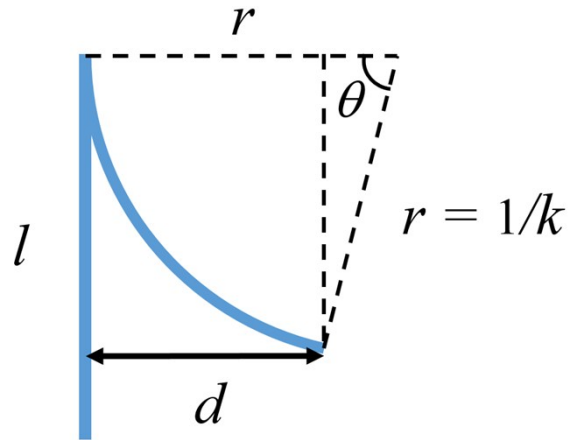


Fig. S3 Schematic of a bimorph actuator with one end fixed bends into an arc.

8. Stability of the PI/AgNW/PDMS actuators

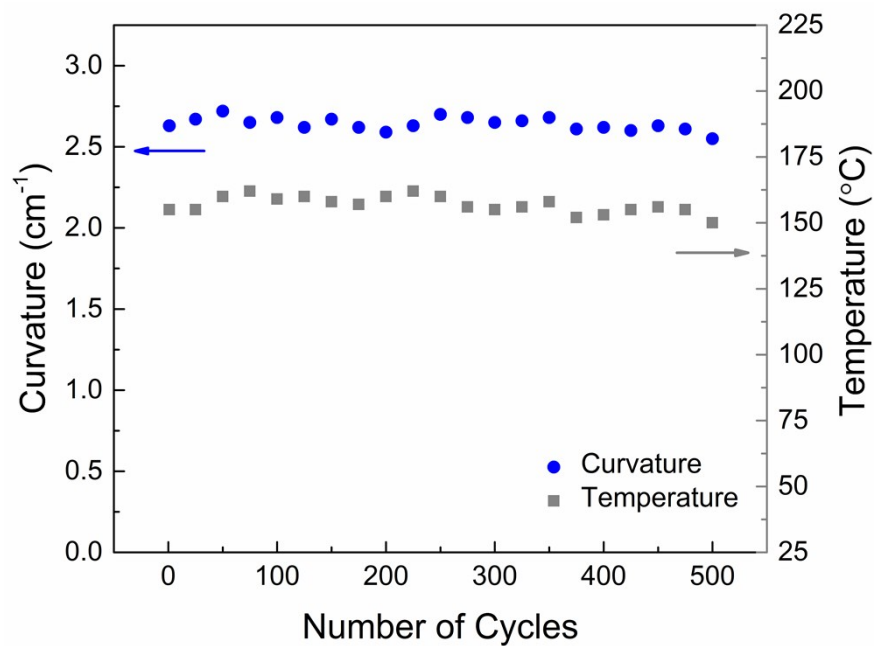


Fig. S4 The changes in temperature and bending curvature with a DC voltage of 4.5 V for up to 500 cycles. The PI/AgNW/PDMS actuators showed reliable performance for up to 500 cycles.

References:

1. L. Chen, C. Liu, K. Liu, C. Meng, C. Hu, J. Wang and S. Fan, *ACS Nano*, 2011, **5**, 1588-1593.
2. Z. Zeng, H. Jin, L. Zhang, H. Zhang, Z. Chen, F. Gao and Z. Zhang, *Carbon*, 2015, **84**, 327-334.
3. L. Chen, M. Weng, W. Zhang, Z. Zhou, Y. Zhou, D. Xia, J. Li, Z. Huang, C. Liu and S. Fan, *Nanoscale*, 2016, **8**, 6877-6883.
4. L. Chen, M. Weng, Z. Zhou, Y. Zhou, L. Zhang, J. Li, Z. Huang, W. Zhang, C. Liu and S. Fan, *ACS Nano*, 2015, **9**, 12189-12196.
5. M. Amjadi and M. Sitti, *ACS Nano*, 2016, DOI: 10.1021/acsnano.1026b05545.
6. Y. Hu, T. Lan, G. Wu, Z. Zhu and W. Chen, *Nanoscale*, 2014, **6**, 12703-12709.
7. J. J. Bae, S. C. Lim, G. H. Han, Y. W. Jo, D. L. Doung, E. S. Kim, S. J. Chae, T. Q. Huy, N. Van Luan and Y. H. Lee, *Adv. Funct. Mater.*, 2012, **22**, 4819-4826.
8. S. Hong, H. Lee, J. Lee, J. Kwon, S. Han, Y. D. Suh, H. Cho, J. Shin, J. Yeo and S. H. Ko, *Adv. Mater.*, 2015, **27**, 4744-4751.
9. S. Ji, W. He, K. Wang, Y. Ran and C. Ye, *Small*, 2014, **10**, 4951-4960.
10. S. Timoshenko, *JOSA*, 1925, **11**, 233-255.
11. DuPont™ Kapton® Polyimide Film Datasheet, (accessed Jan 2016).
12. S. H. Jeong, S. Zhang, K. Hjort, J. Hilborn and Z. Wu, *Adv. Mater.*, 2016, **28**, 5830-5836.
13. C. Bartholome, A. Derré, O. Roubeau, C. Zakri and P. Poulin, *Nanotechnology*, 2008, **19**, 325501.
14. J. Liang, L. Huang, N. Li, Y. Huang, Y. Wu, S. Fang, J. Oh, M. Kozlov, Y. Ma, F. Li, R. Baughman and Y. Chen, *ACS Nano*, 2012, **6**, 4508-4519.
15. W. Jiang, D. Niu, H. Liu, C. Wang, T. Zhao, L. Yin, Y. Shi, B. Chen, Y. Ding and B. Lu, *Adv. Funct. Mater.*, 2014, **24**, 7598-7604.
16. X. Zhang, Z. Yu, C. Wang, D. Zarrouk, J.-W. T. Seo, J. C. Cheng, A. D. Buchan, K. Takei, Y. Zhao, J. W. Ager, J. Zhang, M. Hettick, M. C. Hersam, A. P. Pisano, R. S. Fearing and A. Javey, *Nat. Commun.*, 2014, **5**, 1-8.
17. Y. Jiang, C. Hu, H. Cheng, C. Li, T. Xu, Y. Zhao, H. Shao and L. Qu, *ACS Nano*, 2016, **10**, 4735-4741.